Colloid Polym Sci (2009) 287:167–178
DOI 10.1007/s00396-008-1960-5

ORIGINAL CONTRIBUTION

# Convectional and sedimentation dissipative patterns of Miso soup

**Tsuneo Okubo**

Received: 8 October 2008 / Accepted: 25 October 2008 / Published online: 15 November 2008


**Abstract** Convectional and sedimentation dissipative patterns of Miso soup, one of the traditional Japanese soups, were observed in a Miso soup bowl, a green tea Ochawan (cup), a glass cup, a large glass bowl, and a large watch glass. When Miso soup was set in the substrates, the distorted Benard cells were soon observed after the initial irregular circulations, and the holes grew large at the cross points of the neighboring three Benard cells. The global integrated flow direction of convections at the liquid surface was from the center area toward the outside edge during the periods of formation of the distorted Benard cells. Meanwhile, the reversal of the global flow direction, from outward to inward, at the liquid surface took place. Furthermore, the inward flow at the surface, i.e., the outward flow at the bottom, was accompanied with the broad ring-like sedimentation patterns. The most plausible kinetic scheme of the change in the convectional patterns is proposed in this work.

**Keywords** Miso soup · Convectional pattern · Sedimentation pattern · Dissipative structure · Benard cell

## Introduction

In general, most structural patterns in nature form via self-organization accompanied with the dissipation of free energy and in the non-equilibrium state. In order to know the mechanisms of the dissipative self-organization of the simple model systems instead of the much complex nature itself, the author has studied the convectional, sedimentation, and drying dissipative patterns during the course of drying colloidal suspensions and solutions as systematically as possible, although the three kinds of patterns are correlated strongly and overlapped each other.

Most famous convectional pattern is the hexagonal circulating one, Benard cell, and has been observed when liquids contain plate-like colloidal particles as monitors and are heated homogeneously in a plain pan [1]. Another typical convectional dissipative pattern is the spoke-like lines, which were observed in the whole area of the liquid surface and also appeared in various substrates sometimes accompanied with the huge number of small cell convections. The spoke patterns with cell convections were observed formerly for the membranes of Chinese black ink on water by Terada et al. [2–7]. Authors like to call the spoke-like pattern as Terada cell. The convectional patterns, especially Terada cells, were observed directly in the initial course of dryness of the Chinese black ink in a glass dish [8], the 100% ethanol suspensions of colloidal silica spheres [9], a cup of Miso soup (this work), coffee with cream [10], black tea with cream (Okubo et al., in preparation), and colloidal crystals of poly(methyl methacrylate) (PMMA) colloidal spheres on a cover glass and a watch glass [11, 12]. Distorted Benard cells were often observed for Miso soup, coffee, and black tea. For the 100% ethanol suspensions of colloidal silica spheres, Terada cell-type convectional flow was observed clearly with the naked eyes, and the convectional patterns changed dynamically with time. Quite recently, the whole growing processes of the convectional patterns were observed for coffee with cream [10]. The convectional processes were analyzed as six steps: (1) at the initial stage, the irregular

T. Okubo (✉)
Institute for Colloidal Organization,
Hatoyama 3-1-112,
Uji, Kyoto 611-0012, Japan
e-mail: okubotsu@ybb.ne.jp

T. Okubo
Cooperative Research Center, Yamagata University,
Johnan 4-3-16,
Yonezawa 992-8510, Japan

circulating lines appeared at random in their direction. (2) Global flow of convection at the surface layers at the initial stage was from the center toward the outside edge. Furthermore, (3) the distorted Benard cells were formed at the liquid surface. (4) Meanwhile, at the middle stage of convections, global flow of convection was reversed in direction, from the outside edge to the central area at the liquid surface, and the outward direction remained for a long time until solidification takes place and also induced the broad ring-like sedimentation structure. (5) At the same time, few and short spoke lines appeared at the outside edge. Then, a number of the spoke lines increased. (6) Growth of the spoke lines and formation of the clusters and bundles of the spoke lines took place from the middle to the final stages. The sedimentation and drying patterns were also observed in coffee plus cream suspensions. The bundle patterns at the final stage of convection are considered to be the sedimentation patterns and are further transferred to the drying patterns with fine structures.

Deegan et al. [13, 14] have reported the traces of spoke-like patterns in the suspensions of polystyrene spheres (1 μm in diameter) under a microscope. They introduced the capillary flow theory accompanied with the pinning effect of the contact line of the drying drop. From our series of drying experiments for suspensions and solutions on a cover glass, the pinning effect was not supported except experiments at high particle concentrations and for small colloidal particles. Generally speaking, at high solute concentrations, the broad ring-like drying patterns were always formed irrespective of the substrates used, but they moved toward the central area as their size increased and/or their concentration decreased [8, 15–20]. For typical anisotropic-shaped particles, furthermore, broad rings at the outside edge disappeared and round hill appeared instead [21]. The author believes that the convectional flow of solvent and solutes is essentially important for all the convectional, sedimentation, and drying pattern formation. Furthermore, the pinning effect was not supported in a glass dish where drying frontier starts from the central area of a vessel substrate toward outside [22, 23]. The broad ring drying patterns, however, were not formed at the outside area. Cachile et al. [24, 25] reported that droplets of completely wetting liquids deposited on a perfectly smooth and wetting surface for which no contact line anchoring occurs. It should be mentioned further that theoretical and experimental studies for the convectional patterns have been made intensively hitherto, but these are not always successful yet [11, 13, 14, 24–33]. The main cause for this is the insufficient experimental studies so far. It should be noted further that information on the size, shape, conformation, and/or flexibility of particles and polymers is transformed cooperatively and further accompanied with the amplification and selection processes toward the succeeding sedimentation and drying patterns during the course of dryness of solutions and suspensions.

Sedimentation dissipative patterns in the course of drying suspensions of colloidal silica spheres (183 nm to 1.2 μm in diameter) [17, 18, 34–37], size-fractionated bentonite particles [21], and green tea (Ocha) [38] have been studied in detail in a glass dish, a cover glass, a watch glass, and others, for the first time, in our laboratory. The broad ring patterns were formed within several 10 min in suspension state by the convectional flow of water and the colloidal particles. It was clarified that the sedimentary particles were suspended above the substrate by the electrical double layers and always moved by the balancing of the external force fields including convectional flow and sedimentation. The sharpness of the broad rings was sensitive to the change in the room temperature and/or humidity [36]. The main cause for the broad ring formation is the convectional flow of water and colloidal particles along the cell wall at the lower layers of liquid at the different rates where the rate of the latter is slower than that of the former. Quite recently, it was clarified that the dynamic bundle-like sedimentation patterns formed cooperatively from the distorted spoke line convectional structures of colloidal particles of coffee [10], colloidal crystal suspensions of PMMA spheres [12], and black tea (Okubo, in preparation).

Drying dissipative patterns have been studied for suspensions and solutions of many kinds of colloidal particles [8–12, 15–19, 21, 22, 24–37, 38–51], linear-type synthetic and bio-polyelectrolytes [20, 52], water-soluble and non-soluble neutral polymers [53, 54], ionic and non-ionic detergents [55–57], gels [58], and dyes [59] mainly on a cover glass. The macroscopic broad ring patterns of the hill accumulated with the solutes in the outside edges formed on a cover glass, a watch glass, and a glass dish when the solute concentration was high. However, the broad rings moved inward when solute concentration decreased and/or solute size increased. For the non-spherical particles, furthermore, the round hill was formed in the central area in addition to the broad ring [21]. Macroscopic spoke-like cracks or fine hills, including flickering spoke-like ones, were also observed for many solutes. Furthermore, beautiful fractal patterns such as earthworm-like, branch-like, arc-like, block-like, star-like, cross-like, and string-like ones were observed in the microscopic scale. These microscopic drying patterns were often reflected from the shape, size, and/or flexibility of the solutes themselves. Microscopic patterns also formed by the translational Brownian diffusion of the solutes and the electrostatic and/or the hydrophobic interactions between solutes and/or between the solutes and the substrate in the course of the solidification. One of the very important findings in our experiments is that the primitive vague

sedimentation patterns were formed already in the liquid phase before dryness and they grew toward fine structures in the process of solidification [21].

In this work, convectional and sedimentation dissipative patterns of Miso soup, one of the traditional Japanese soups, have been observed on the macroscopic and microscopic scales. Surprisingly, the reversal of the total flow of the particles from the outer toward the inner one was observed with the naked eyes. This reversal has been observed for coffee with cream for the first time [10]. Furthermore, distorted Benard cells and broad ring-like sedimentation patterns were observed in the beginning and final stages of convections, respectively, in this work. The convectional processes are proposed in general in this work.

## Experimental

### Materials

Two kinds of Miso pastes for home use in Japan (type I, malted rice miso, Marusanai, Okazaki) and an instant Miso soup (type II, Nagatanien, Tokyo) were utilized. Compositions of the type I Miso paste are water (42.6 wt.%), protein (9.7%), lipid (3.0%), fatty acid (2.9%), carbohydrate (38%), dietary fiber (5.6%), and an equivalent amount to NaCl (6.1%) [60]. On the other hand, type II Miso paste is composed of water (41.6 wt.%), protein (15.7%), lipid (7.4%), fatty acid (2.9%), carbohydrate (20.5%), dietary fiber (2.7%), and an equivalent amount to NaCl (9.2%) as reported by the manufacturer. The shape of Miso particles are highly polydispersed plate-like for both types of Miso paste. Their size ranges from approximately 10 μm to approximately 1.8 mm and from approximately 10 μm to 1 mm for types I and II, respectively. Miso soup type I was prepared by dilution of these pastes with boiled water, including several ingredients such as onion, potato, and tofu, for example in a pan in the processes of cooking. All of the ingredients were removed from the Miso soup in a bowl using chopsticks before observation. Miso soup type II was prepared by dilution of the paste with boiled water directly using chopsticks. Tap water of Uji city (Kyoto) was used for the preparation of Miso soup.

### Observation of the dissipative structures

Type I Miso soup (about 180 ml) was poured into a Miso soup bowl made of lacquered wood (130-mm outside diameter, 77-mm height). Type II Miso paste (18.7 g) in an aluminum foil bag and 180 ml of boiled water were put into a Miso soup bowl made of plastics (115-mm upper outside diameter, 60-mm height). An Ochawan (green tea cup) was made of clay, 90 mm in outside diameter and 51 mm in height. A medium glass cup of flat bottom was 85 mm in diameter and 63 mm in height. A large glass bowl having the gently round inner bottom was a microwavable Pyrex (140-mm outside diameter, Iwaki, Tokyo). Type II Miso soup (40 ml) was also set on a large watch glass (150-mm diameter, TOP, Tokyo). Most of the convectional and sedimentation patterns were observed for the suspensions on a desk covered with a black plastic sheet. Bottom view pictures were also taken for a large glass bowl. The room temperature was regulated at 25 °C. However, humidity of the room was not regulated and is between 45% and 60%.

Macroscopic patterns were observed on a Canon EOS 10 D digital camera with a macro-lens (EF 50 mm, $f$=2.5) and a life-size converter EF. Canon digital camera IXY-digital 80 was also used for the macroscopic observation including video pictures.

### Measurements of change in the temperature of boiled water in the various vessels

The boiled water instead of the actual Miso soup was poured into the Miso soup bowl, green tea cup, middle size glass cup, large glass bowl, and large watch glass. The water temperatures at the high layers close to the air–water surface, at the low layers close to the liquid bottom, and further at the high layers around the outside area if possible were measured on a digital thermometer (model SK-250WPII-N, Sato Gauge, Tokyo) with a sensor stick (type SWPII-01M, Sato Gauge). The point top of the stick (f3× 100 mm in length, made of rustproof steel SUS304) encloses a thermistor. The sensitivity of the measuring temperature is ±0.3 °C. The thermo-sensitive area of the sensor stick top is considerably wide (approximately 2×2× 2 mm), and the pinpoint measurements of the liquid are difficult.

## Results and discussion

### Convectional and sedimentation patterns of Miso soup in a Miso soup bowl

Figure 1a shows a typical example of convectional patterns of Miso soup (type I) in a Miso soup bowl. Several important findings are clear in the pictures. Firstly, the distorted Benard cells grew up especially within 30 s after the suspension was set. Hexagonal patterns are clear. Colloidal particles of Miso soup are highly polydispersed in their size and shape. However, flow birefringence, which affects the multiple scattering, is very strong. This high flow birefringence effect will be the main reason why the distorted Benard cells were observed with the naked eyes. It should be mentioned here that the distorted Benard cells

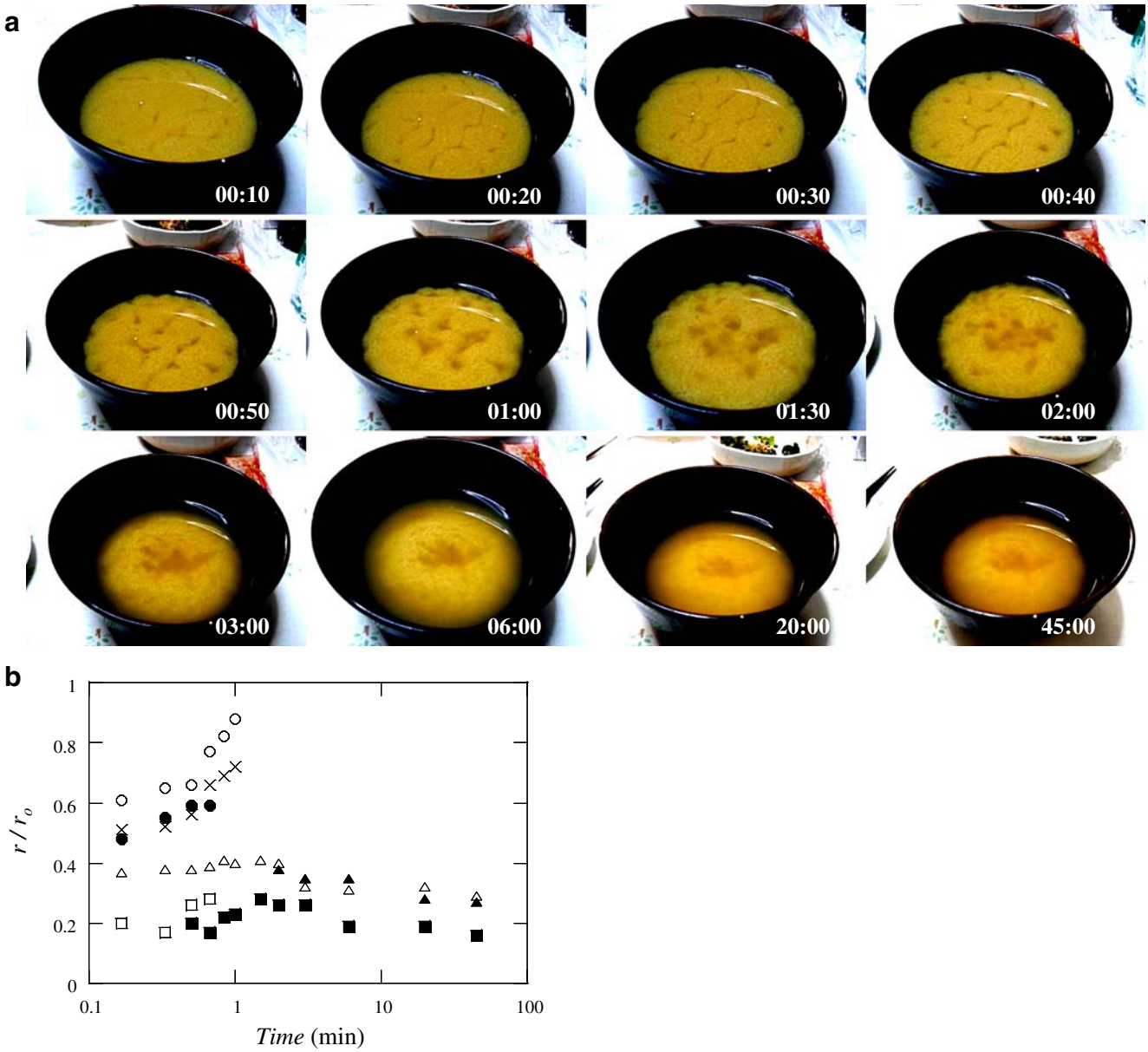


**Fig. 1** **a** Convectional patterns of type I Miso soup in a bowl from approximately 60 °C to 30 °C. Experiment 1, time (minutes:seconds). Miso I=0.06 g/ml, 180 ml. **b** The $r/r_o$ plots against time elapsed for typical points shown in **a**

have been seldom observed hitherto. The author has observed only for Chinese black ink in a glass dish [8] and coffee with cream [10]. On the other hand, Terada cells, i.e., the spoke-line pattern formed on the whole liquid surface, were often observed for Chinese black ink in a glass dish [8], colloidal crystals of poly(methyl methacrylate) spheres on a cover glass and a watch glass [11, 12], and coffee with cream [10] for example. However, the Terada cells were not observed in Fig. 1a. Secondly, in the beginning stage of convection from 30 s to 1 min, the holes formed and grew large at the cross points of the neighboring three Benard cells. The Miso colloidal particles rise up at the central area of each Benard cells and flowed down at the outside edges especially at the holes sharply. Furthermore, the holes moved slowly toward outside first as is shown in the movement of the right-hand side two holes within 1 min after setting.

Thirdly, the enlarged holes came together at a time between 1 and 6 min. Reversal of the flow direction of the holes between 1 and 2 min after setting is clearly shown in Fig. 1b. Here, the distances of the typical seven holes from the center ($r$) against the radius of the liquid surface ($r_o$), $r/r_o$ values, were plotted as a function of time elapsed. The reversal of the convectional flow at the liquid surface took place clearly during 1 to 2 min after setting. When the hot suspensions were set in the substrates, very rapid circu-

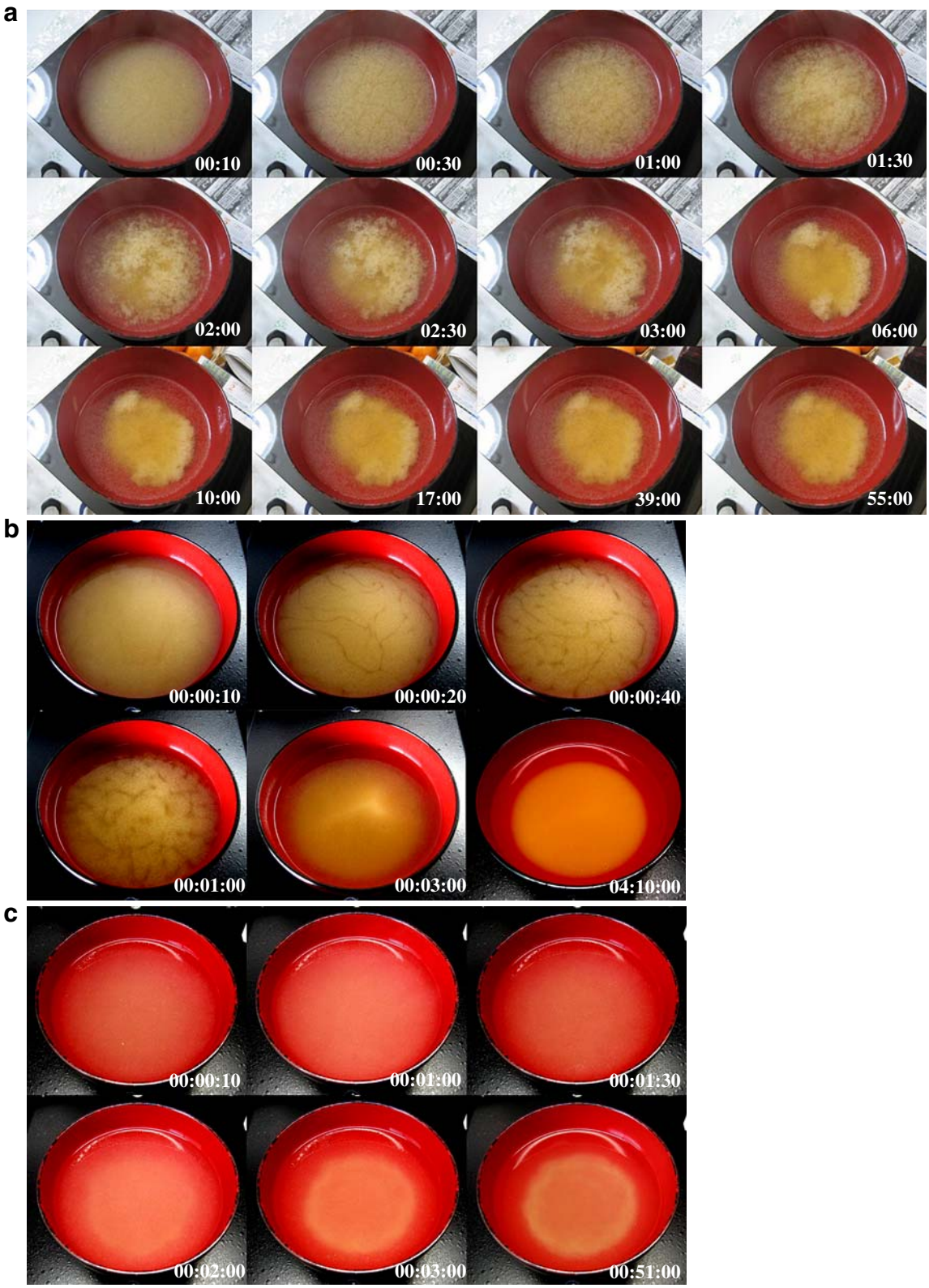


**Fig. 2** **a** Convectional patterns of type I Miso soup in a bowl from approximately 50 °C to 25 °C. Experiment 8, time (minutes:seconds). Miso I=0.06 g/ml, 180 ml. **b** Convectional patterns of type II Miso soup in a bowl from approximately 60 °C to 30 °C. Experiment 3, time (minutes:seconds), Miso II=0.030 g/ml, 180 ml. **c** Convectional patterns of type II Miso soup in a bowl from approximately 60 °C to 30 °C. Experiment 4, time (minutes:seconds). Miso II=0.0051 g/ml, 180 ml

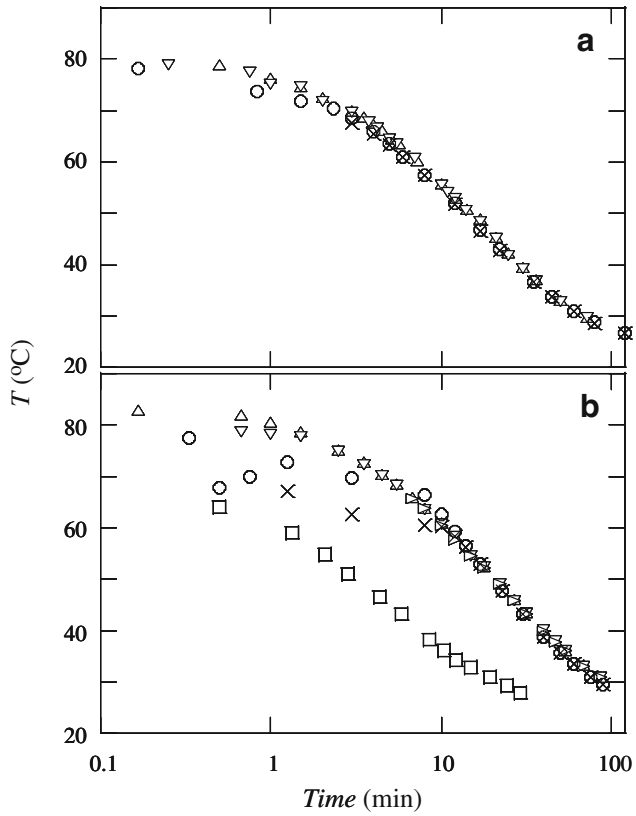


**Fig. 3** **a** Change of boiled water temperature with time in a Miso soup bowl (*circle*: high in the water layers close to the surface, *ex*: low layers close to the bottom) and a green tea cup (*triangle*: high, *inverted triangle*: low) at 26 °C. **b** Change of suspension temperature in a medium glass cup (*circle*: high, *ex*: low), a large glass bowl (*triangle*: high, *inverted triangle*: low, *right triangle*: high, side), and a large watch glass (*square*) at 26 °C

lations will take place by the gravitational buoyancy effect. Then, the temperature gradient is formed where temperatures of the upper and lower layers of the suspensions are high and low, respectively. When these gradients are formed stably, the reversal of the global flow of suspensions should take place by the Marangoni effect from the top toward bottom especially at the central area of the liquid. The detailed discussion on the reversal is described below. The reversal of the convectional flow has been also observed for coffee plus cream [10]. Clearly, growth of the distorted hexagonal Benard cells was always accompanied with the outward total flow at the liquid surfaces. On the other hand, the reversed inward flow is accompanied with the formation of a large hole at the central area and, further, a broad ring-like sedimentation patterns. In other words, the broad ring sedimentation patterns are formed mainly by the outward total flow of the colloidal particles in the lower layers of liquid. The broad ring-like sedimentation patterns were formed by the balancing between the outward (or upward) flow of convection in the lower layers of liquid and the inward (or downward) flow of the sedimentation of the colloidal particles on a cover glass or a watch glass, respectively [17, 18, 21, 34–38].

Figure 2a shows another example of observation of Miso soup (type I) in a bowl. Here, the slow rotation of the patterns took place at the liquid surface. However, the distorted Benard cells were observed again (see the pictures 30 s to 1 min after setting). In this observation, the sedimentation of the Miso colloids took place fast at a first glance. However, it was clearly observed with the naked eyes that the downward flow of the colloids that took place at the outside edge of the liquid was clear in the beginning stage between 10 s to 1 min. Surprisingly, the reversal of the convectional flow, i.e., the upward flow around the outside edges, was soon observed with the naked eyes at the middle stage of convections from 01:30 to 06:00. Furthermore, pictures from 01:30 to 06:00 demonstrate the processes of the broad ring-like sedimentation patterns clearly. The importance of the inward and outward flows of convection at the liquid surface and then the reversed flow at the bottom layers is clear for the broad ring formation as demonstrated by these pictures. It should be mentioned here that within 10 s after the suspension was set, the circulation was quite irregular. During this time, the vigorous vertical gravitational buoyancy flow of suspension is highly plausible.

Figure 2b,c shows the other typical examples of the convectional patterns with time at high and low particle concentrations of type II Miso soup, respectively. The slow rotation of the patterns again took place in Fig. 2b. The irregular circulations took place within 10 s. The formation and further growth processes of the distorted Benard cells were observed at 00:00:20 and 00:00:40. Furthermore, the enlarging processes of the holes are clear from a comparison of two pictures, 00:00:40 and 00:01:00. Observation of the broad ring-like sedimentation pattern was observed vaguely but is not so clear (see the pictures of 04:10:00). This is due to the fact that the particle concentration was high enough to show the yellowish colors on the whole pattern area by the strong effect of multiple scattering of light. When the particle concentration was low, on the other hand, the broad ring sedimentation pattern was observed clearly (see the pictures 00:03:00 and 00:51:00 in Fig. 2c). The distorted Benard cells were not recognized at all for the diluted suspensions instead.

It should be discussed here why the flow reversal takes place more in detail. Figure 3 shows the temperature change in the process of cooling the boiled water with time elapsed in the several substrates. Here, the abscissa is time in logarithm scale. Several important findings are made in the figure. Firstly, the temperature during the initial around 1 min was quite unstable and changed sharply depending on time and location. Secondary, around 1 min after setting, the stable distribution of the temperatures

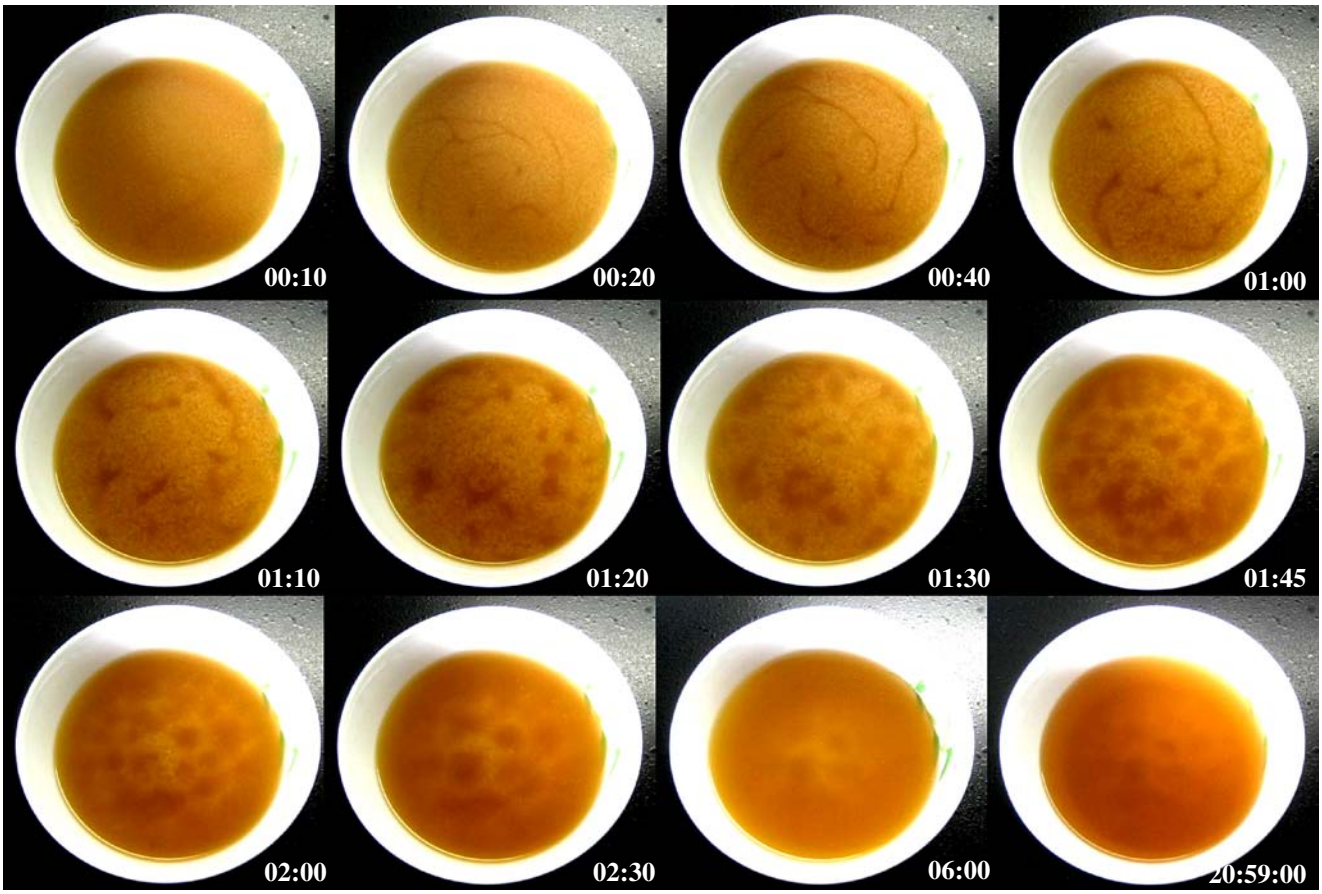


**Fig. 4** Convectional patterns of type II Miso soup in a tea cup (Ochawan) from approximately 40 °C to 20 °C. Experiment 6, time (minutes: seconds or hours:minutes:seconds; lowest right flame). Miso II=0.038 g/ml, 100 ml

was formed depending on the locations measured in the order:

$$[\text{High and central area}] > [\text{high and outside area}] > [\text{low and central area}]. \quad (1)$$

Measurements of the temperature of the thin liquid at the air–water surface were impossible in this work. However, it is highly plausible that the thin liquid temperature after 1 min is lower than those at all the spots measured. Thus, the temperatures will be distributed depending on the location as follows:

$$[\text{High and central}] > [\text{high and outside}] > [\text{low and central}] > [\text{highest thin liquid}]. \quad (2)$$

Let us discuss the flow direction of water mainly at the central area qualitatively. During about one to several minutes, vigorous evaporation of water molecules from the liquid surface will introduce the lowering of the temperature of the thin liquid at the surface accompanied with the upward flow by the Marangoni convectional force between the thin liquid and bulk liquid. Gravitational (buoyant) convection also introduces the upward flow of water in the bulk. This temperature gradient in the liquid is kept for a while, since the heat is absorbed through the bottom wall of the vessel continuously. Furthermore, the thermocapillary convectional flow will be introduced in the direction from the center toward outside edge in the high layers of liquid, since the temperature at the outside area is low compared to that at the center [61, 62]. Thus, the global flow of liquid is a circling upward flow in the center followed by the outward flow to outside edge at the high layers of liquid, as is shown in the top right of Fig. 8. After several minutes, the distribution of temperature depending on the locations will be established, where temperatures at the high and low liquid layers are high and low, respectively. This temperature gradient will induce the Marangoni flow in the lower direction during the course of cooling of the liquid. Furthermore, the upward buoyant flow at the central area will be weakened sharply, since the liquid temperature is lowered down. Thus, the downward flow in the liquid bulk should take place in preference instead, as is shown in Fig. 8, indicated by "global flow reversed". This reversal in the direction of the convectional flow at the central area will be the main reason why the flow inversion takes place. It should be

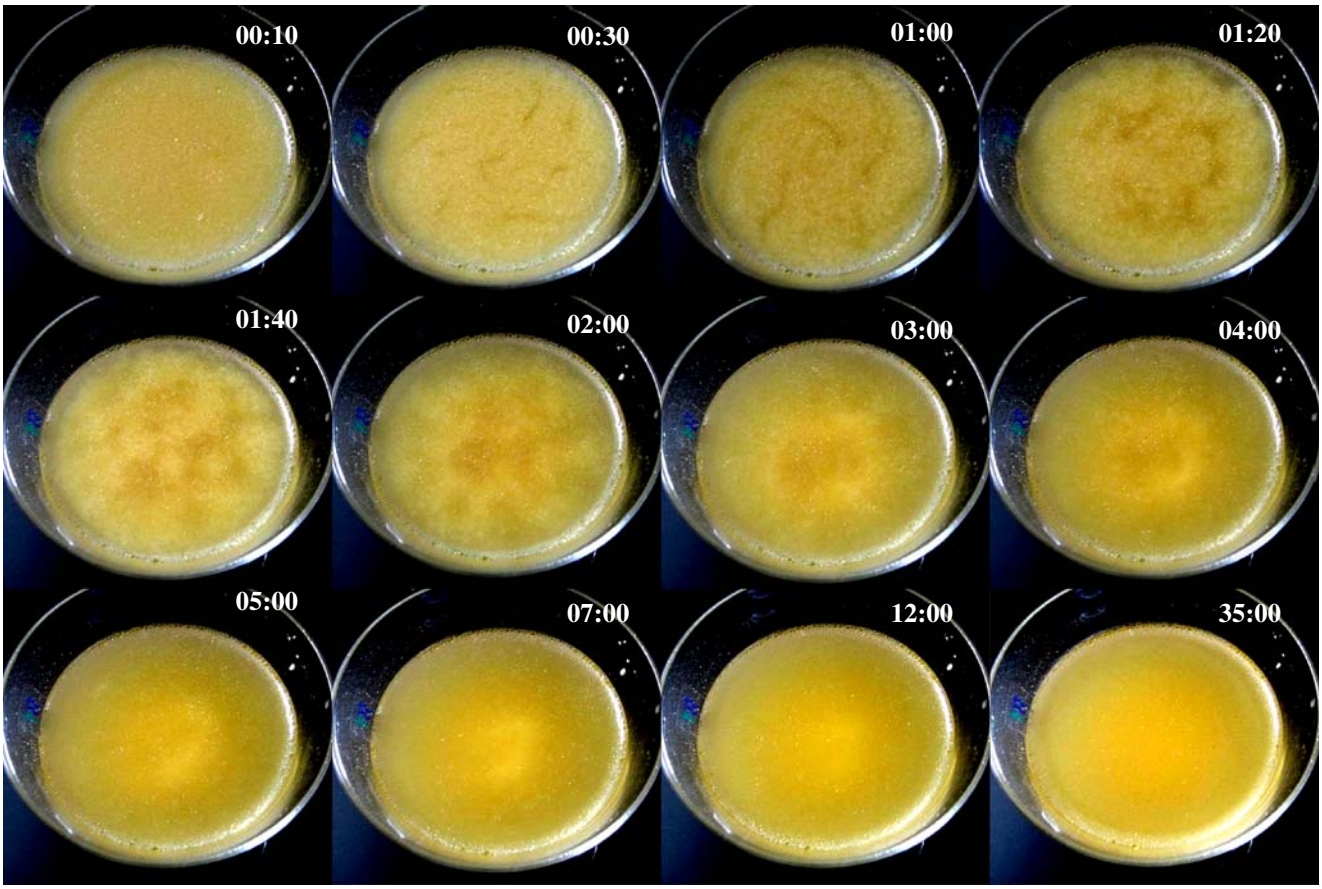


**Fig. 5** Convectional patterns of type II Miso soup in a medium glass bowl from approximately 50 °C to 25 °C. Experiment 7 (minutes:seconds). Miso II=0.061 g/ml, 100 ml

noted here that the distorted Benard cells and Terada cells are formed during the periods of initial global flow and the reversed global flow, respectively, as is shown schematically in Fig. 8. It should be noted here that an important role of the Marangoni flow induced by a gradient in temperature at the liquid surface and also of the relative thermal conductivities of the substrate and liquid were proposed for the circulation reversal in evaporating drops on a plane substrate [63, 64].

Broad ring-like sedimentation patterns were formed after Miso soup was kept for a long time, as is shown in Figs. 1a, and 2a,c, for example. These sedimentation patterns were formed by the balancing between the upward (or outward) convectional flow and downward (or inward) sedimentation in the Miso soup bowl [17, 18, 34–38].

## Convectional and sedimentation patterns of Miso soup in a green tea cup, a middle size glass cup, and a large glass bowl

Figure 4 shows the convectional patterns of Miso soup (type II) in an Ochawan (a cup for taking green tea). Here, during the initial 10 s, irregular circulations took place. However, highly distorted Benard cells were observed after approximately 20 s, although the liquid surface rotated slowly clockwise in the pictures. Furthermore, the holes grew at the cross points of the neighboring three Benard cells between 1 and 2 min, and further, the grown-up holes moved outward first (between 1 and 1 min, 45 s) and then turned to move inward (see 01:45 to 06:00). These features of the change in the convectional patterns are quite similar to those in the Miso soup bowls.

A typical example of the convectional patterns of Miso soup in a medium size glass cup is shown in Fig. 5. Here, the quite similar events of the convectional patterns to those in Ochawan in Fig. 4 are shown: the formation of the distorted Benard cells and outward and then inward global flow of the patterns at the liquid surface, although the patterns were vague by the light scattering of the oil layers at the liquid surface. In Fig. 5, the fried tofu (“Oage” or “Abura-age”) was one of the gradients of the Miso soup.

Figure 6a–c shows the top view of the convectional patterns as a function of time elapsed in a large glass bowl. In Fig. 6a, the formation processes of the distorted Benard cells, the holes and the broad rings, are recognized with the naked eyes. Figure 6b,c shows the bottom view of the convectional

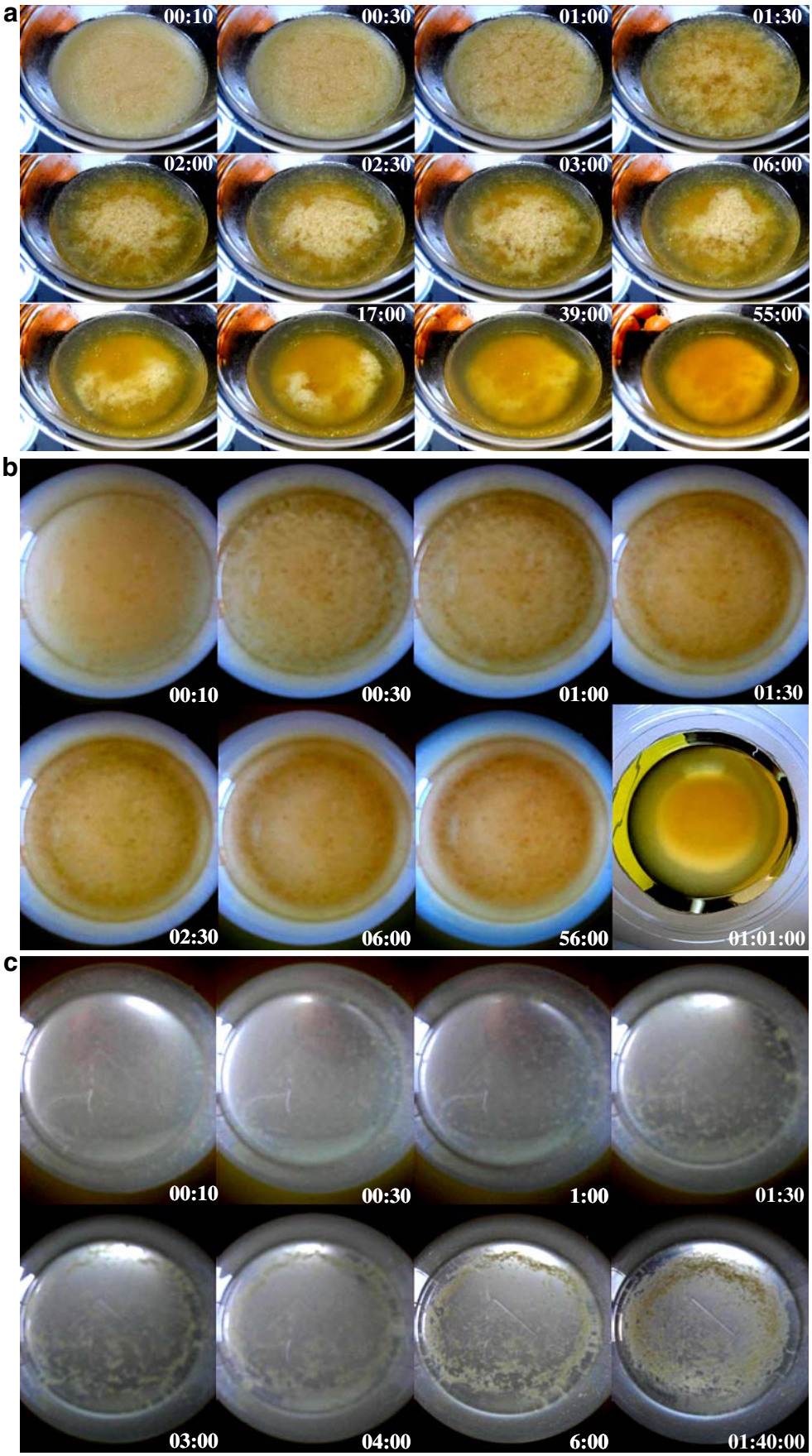


**Fig. 6** **a** Convectional patterns of type II Miso soup in a large glass bowl from approximately 50 °C to 20 °C. Experiment 7, time (minutes:seconds). Miso II=0.061 g/ml, 270 ml. **b** Convectional patterns of type II Miso soup in a large bowl from approximately 60 °C to 25 °C. Experiment 9, bottom view except lowest right flame, up view, time (minutes:seconds or hours: minutes:seconds; lowest right flame). Miso II=0.0061 g/ml, 270 ml. **c** Convectional patterns of type II Miso soup in a large bowl from approximately 60 °C to 25 °C. *Bottom view*, time (minutes:seconds or hours: minutes:seconds; lowest right flame). Miso II=0.0020 g/ml, 270 ml

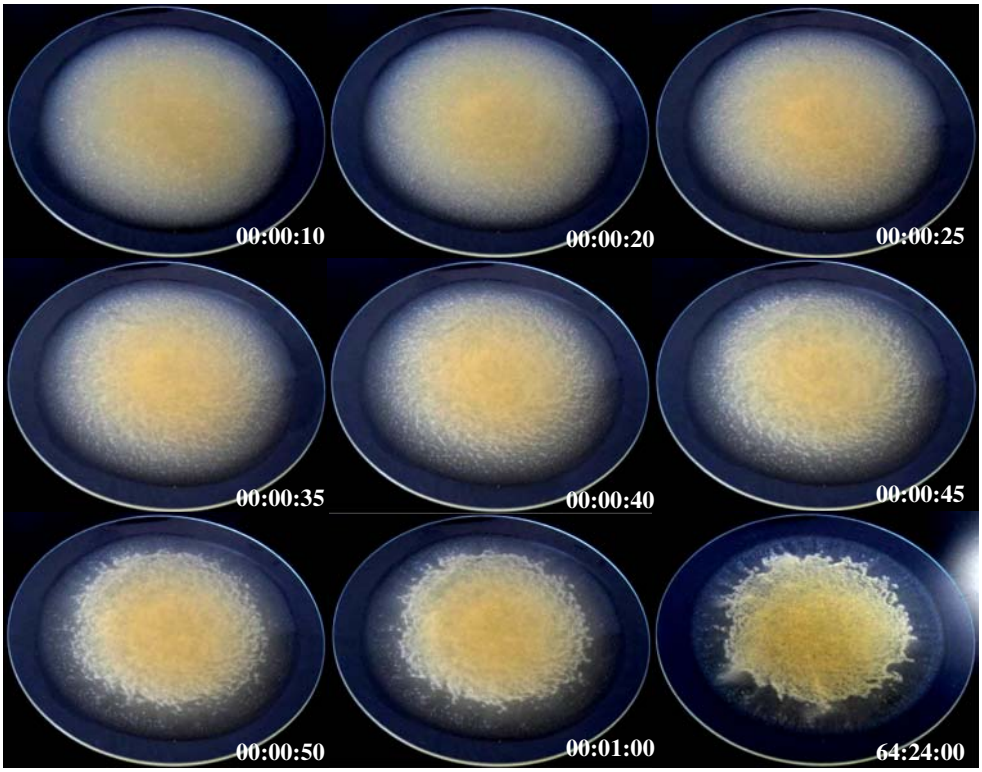


**Fig. 7** Convectional patterns of type II Miso soup in a large watch glass from approximately 60 °C to 40 °C. Experiment 10, time (hours:minutes:seconds). Miso II=0.061 g/ml, 40 ml

patterns of the diluted Miso soups, one tenth and one thirtieth, respectively. In Fig. 6b, both the distorted Benard cells and the global flow of the patterns were not observed. These are presumably due to the fact that the Benard cells are formed at the liquid surface and the preferential fall of very large Miso particles on the bottom takes place and disturbs the convectional flows at the higher layers. The broad ring formation was observed clearly for the diluted suspension (see the pictures 01:00 to 56:00) especially in Fig. 6c. However, the distorted Benard cells and the global flow of the patterns were not observed again in Fig. 6c.

## Convectional and sedimentation patterns of Miso soup in a large watch glass

Figure 7 shows a typical example of the change in the convectional and sedimentation patterns of Miso soup (type II). Pattern change was very fast in a watch glass, and all the processes from convectional to sedimentation patterns completed within 1 min. This will be due to the fact that the depth of the liquid is thin compared to the cups and bowls used above. The patterns at the surface of the liquid rotated clockwise and slowly in this case too. Distorted Benard

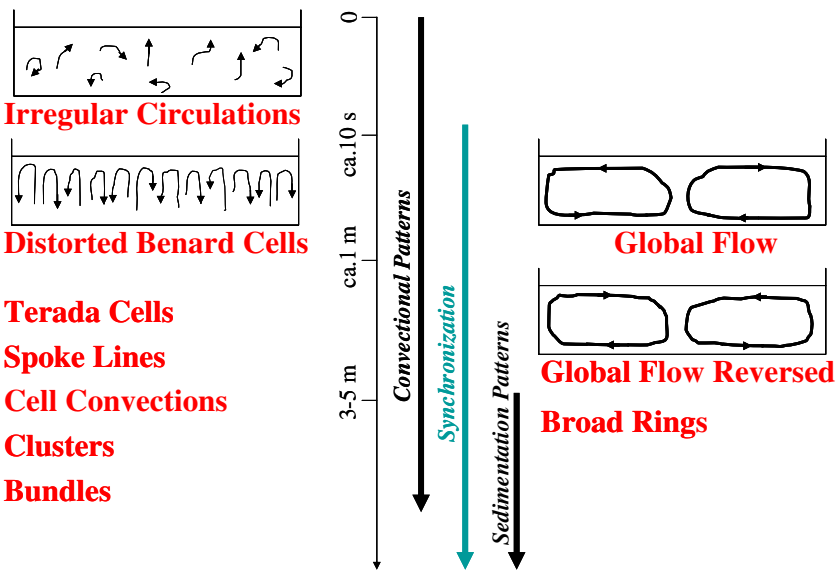


**Fig. 8** Most plausible kinetic scheme of convectional patterns. Time scale is given for Miso-soup of this work

cells did not appear in this case. However, the figure shows the processes of the formation of spoke lines around the outside area of the patterns. The broad ring-like sedimentation patterns are also observed in the pictures 00:00:50 to 64:24:00 in the figure. The patterns support that the lines were formed by the convectional forces from the outside edge toward center at the liquid surface.

It should be mentioned here that the clusters and the bundles, which were formed for coffee with cream [10] and colloidal crystals of poly(methyl methacrylate) spheres [12] on a watch glass and a cover glass, were not recognized for the Miso soup. This will be due to the fact that the colloidal particles of Miso soup were large and polydispersed. Furthermore, the sedimentation took place within a short time, and then the sufficient time for the cooperative interaction of the neighboring spoke lines was not left.

## Concluding remarks

In this work, the growing processes of the convectional patterns were mainly studied from the macroscopic and microscopic pattern observation of Miso soup on the various substrates. The convectional and sedimentation patterns from the irregular circulating lines, distorted Benard cells, and to the broad rings were observed (see scheme shown in Fig. 8). The convectional processes are analyzed as six steps: (1) at the initial stage, the irregular circulating lines appeared at random in their direction. (2) Global flow of convection at the surface layers at the initial stage was from the center toward outside edge. (3) Furthermore, the distorted Benard cells formed at the liquid surface. (4) Meanwhile, at the middle stage of convections, global flow of convection was reversed in direction from outside edge to the central area at the liquid surface, and the outward direction remained for a long time until solidification takes place and also induced the broad ring-like sedimentation structure. (5) At the same time, few and short spoke lines appeared at the outside edge. Then, the number of the spoke lines increased and grew toward the center. (6) Growth of the spoke lines and formation of the clusters and bundle took place from the middle to the final stages. In the present work, however, the clusters and the bundles were not observed. This will be due to the fact that the colloidal particles of Miso soup were large and polydispersed and the sufficient time for the cooperative formation of clusters and bundles was not left. The broad ring sedimentation patterns were also observed in Miso soup.

**Acknowledgments** Financial supports from the Ministry of Education, Culture, Sports, Science and Technology, Japan and Japan Society for the Promotion of Science are greatly acknowledged for Grants-in-Aid for Exploratory Research (17655046) and Scientific Research (B) (18350057). Professor Akira Tsuchida of Gifu University is thanked for his continuous discussion on the scheme of the convectional patterns.

## References

1. Benard H (1900) Rev Gen Sci Pure Appl 11:1261, 1309
2. Terada T (1928) Rep Aeronaut Res Inst 3:110
3. Terada T, Tamano M (1929) Rep Aeronaut Res Inst 4:51
4. Terada T, Yamamoto R, Watanabe T (1934) Sci Paper Inst Phys Chem Res Jpn 27:173; Proc Imper Acad Tokyo 10:10
5. Terada T, Yamamoto R, Watanabe T (1934) Sci Paper Inst Phys Chem Res Jpn 27:75
6. Terada T, Yamamoto R (1935) Proc Imper Acad Tokyo 11:214
7. Nakaya U (1947) Memoirs of Torahiko Terada (Japanese). Kobunsya, Tokyo
8. Okubo T, Kimura H, Kimura T, Hayakawa F, Shibata T, Kimura K (2005) Colloid Polym Sci 283:1
9. Okubo T (2006) Colloid Polym Sci 285:225
10. Okubo T, Okamoto J, Tsuchida A (2008) Colloid Polym Sci doi:10.1007/s00396-008-1947-2
11. Okubo T, Okamoto J, Tsuchida A (2008) Colloid Polym Sci 286:1123
12. Okubo T (2008) Colloid Polym Sci 286:1307
13. Deegan RD, Bakajin O, Dupont TF, Huber G, Nagel SR, Witten TA (1997) Nature 389:827
14. Deegan RD, Bakajin O, Dupont TF, Huber G, Nagel SR, Witten TA (2000) Phys Rev E 62:756
15. Okubo T, Okuda S, Kimura H (2002) Colloid Polym Sci 280:454
16. Okubo T, Kimura K, Kimura H (2002) Colloid Polym Sci 280:1001
17. Okubo T, Okamoto J, Tsuchida A (2008) Colloid Polym Sci 286:385
18. Okubo T, Okamoto J, Tsuchida A (2008) Colloid Polym Sci 286:941
19. Okubo T, Yamada T, Kimura K, Tsuchida A (2005) Colloid Polym Sci 283:1007
20. Okubo T, Onoshima D, Tsuchida A (2007) Colloid Polym Sci 285:999
21. Yamaguchi T, Kimura K, Tsuchida A, Okubo T, Matsumoto M (2005) Colloid Polym Sci 283:1123
22. Okubo T (2008) Colloid Polym Sci 286:1411
23. Okubo T (2008) Colloid Polym Sci 286:1527
24. Cachile M, Benichou O, Cazabat AM (2002) Langmuir 18:7985
25. Cachile M, Benichou O, Poulard C, Cazabat AM (2002) Langmuir 18:8070
26. Palmer HJ (1976) J Fluid Mech 75:487
27. Anderson DM, Davis SH (1995) Phys Fluids 7:248
28. Pouth AF, Russel WB (1998) AIChE J 44:2088
29. Burelbach JP, Bankoff SG (1998) J Fluid Mech 195:463
30. Matar OK, Craster RV (2001) Phys Fluids 13:1869
31. Hu H, Larson RG (2002) J Phys Chem B 106:1334
32. Rabani E, Reichman DR, Geissler PL, Brus LE (2003) Nature 426:271
33. Fischer BJ (2002) Langmuir 18:60
34. Okubo T (2006) Colloid Polym Sci 284:1191
35. Okubo T (2006) Colloid Polym Sci 284:1395
36. Okubo T, Okamoto J, Tsuchida A (2007) Colloid Polym Sci 285:967
37. Okubo T (2007) Colloid Polym Sci 285:1495
38. Okubo T (2006) Colloid Polym Sci 285:331
39. Vanderhoff JW (1973) J Polym Sci Symp 41:155
40. Nicolis G, Prigogine I (1977) Self-organization in non-equilibrium systems. Wiley, New York
41. Ohara PC, Heath JR, Gelbart WM (1997) Angew Chem 109:1120
42. Maenosono S, Dushkin CD, Saita S, Yamaguchi Y (1999) Langmuir 15:957
43. Nikoobakht B, Wang ZL, El-Sayed MA (2000) J Phys Chem 104:8635
44. Ung T, Litz-Marzan LM, Mulvaney P (2001) J Phys Chem B 105:3441

45. Okubo T, Kanayama S, Kimura K (2004) Colloid Polym Sci 282:486
46. Okubo T (2006) In: Stoylov SP, Stoimenova MV (eds) Molecular and colloidal electro-optics. Taylor & Francis, New York, p 573
47. Okubo T, Nozawa M, Tsuchida A (2007) Colloid Polym Sci 285:827
48. Okubo T, Kimura K, Tsuchida A (2007) Colloids Surf B Biointerfaces 56:201
49. Okubo T, Nakagawa N, Tsuchida A (2007) Colloid Polym Sci 285:1247
50. Okubo T (2008) Nanoparticles: syntheses, stabilization, passivation and functionalization (edited by Nagarajan R, Hatton TA), chapter 19. ACS Book, Washington, DC, p 256
51. Okubo T, Kimura K, Tsuchida A (2008) Colloid Polym Sci 286:621
52. Okubo T, Kanayama S, Ogawa H, Hibino M, Kimura K (2004) Colloid Polym Sci 282:230
53. Shimomura M, Sawadaishi T (2001) Curr Opin Coll Interface Sci 6:11
54. Okubo T, Yamada T, Kimura K, Tsuchida A (2006) Colloid Polym Sci 284:396
55. Okubo T, Kanayama S, Kimura K (2004) Colloid Polym Sci 282:486
56. Kimura K, Kanayama S, Tsuchida A, Okubo T (2005) Colloid Polym Sci 283:898
57. Okubo T, Shinoda C, Kimura K, Tsuchida A (2005) Langmuir 21:9889
58. Okubo T, Itoh E, Tsuchida A, Kokufuta E (2006) Colloid Polym Sci 285:339
59. Okubo T, Yokota N, Tsuchida A (2007) Colloid Polym Sci 285:1257
60. Ministry of Education, Culture, Sports, Science and Technology, Japan (2005) Standard tables of food composition in Japan. Pine System Co., Kumamoto
61. Davis SH (1987) Annu Rev Fluid Mech 19:403
62. Schatz MF, Neitzel GP (2001) Annu Rev Fluid Mech 33:93
63. Hu H, Larson RG (2006) J Phys Chem B 110:7090
64. Ristenpart WD, Kim PG, Domingues C, Wan J, Stone HA (2007) Phys Rev Lett 99:234502